CoCO2

Prototype system for a Copernicus CO_2 service

D3.5 Towards multi-tracer data assimilation capacity for CO_2-MVS

Anne-Wil van den Berg, Wouter Peters, Maarten Krol

Co-ordinated by ECMWF

CoCO2

Prototype system for a Copernicus CO_2 service

D3.5 Towards multi-tracer data assimilation capacity for CO_2-MVS

Dissemination Level:	Public/ Confidential
Author(s):	Anne-Wil van den Berg, Wouter Peters, Maarten Krol (Wageningen Univ)
Date:	21/12/2023
Version:	0.3
Contractual Delivery Date:	31/12/2023
Work Package/ Task:	WP3/T3.4
Document Owner:	Wageningen University
Contributors:	Wageningen University
Status:	**Draft**/ for Review/ Final

$CoCO_2$: Prototype system for a Copernicus CO_2 service

Coordination and Support Action (CSA)
H2020-IBA-SPACE-CHE2-2019 Copernicus evolution – Research activities in support of a European operational monitoring support capacity for fossil CO_2 emissions

Project Coordinator: Dr Richard Engelen (ECMWF)
Project Start Date: 01/01/2021
Project Duration: 36 months

Published by the $CoCO_2$ Consortium

Contact:
ECMWF, Shinfield Park, Reading, RG2 9AX,
richard.engelen@ecmwf.int

The $CoCO_2$ project has received funding from the European Union's Horizon 2020 research and innovation programme under grant agreement No 958927.

Table of Contents

Figures

Tables

1 Executive Summary

The global CO_2 Monitoring Verification System (CO_2 MVS) of the Copernicus CO_2 Service will track emissions of greenhouse gases caused by human activity. This includes the combustion of fossil fuels which dominates the carbon balance of many developed countries, but also emissions caused by land-use, land-use change, and forestry (LULUCF). In many countries rich in forests or peatlands, or in countries intensifying their agricultural production, carbon emissions from managing the land are at least as large as those by combustion of fossil fuels. Most of those countries share two important features: the first is that deforestation is a large and visible problem resulting in large carbon release, the second is that these emissions are poorly known and national legislation is hampered by a lack of national registration and monitoring. This convergence signifies a great opportunity for Copernicus' CO_2MVS to contribute independent, timely, and actionable information to stakeholders worldwide.

This Deliverable sketches the contours of a framework to further exploit satellite observations of atmospheric species in the CO_2MVS, specifically aimed at determining emissions from deforestation. It builds on previous work in our community which has demonstrated the large added value of carbon monoxide (CO) as a tracer for combustion of biomass. We present and evaluate a modelling framework in which the budgets of CO_2 and CO are fully coupled, enabling observation-based optimisation of fire carbon emissions which are often linked to land use change. In the current system, these emissions are constrained only by Fire Radiative Power (FRP) through the Global Fire Assimilation System (GFAS), as part of both CAMS and the CO_2MVS. To highlight the processes that are important in a future system, we focused our work on a two-month period of unexpectedly large deforestation emissions in the Amazon in 2019, when observations from multiple platforms (OCO-2, TROPOMI, MOPITT, IASI, TCCON, ATTO, Amazon aircraft profiles, NOAA flasks) were available to us.

Based on the work performed in $CoCO_2$ and under parallel efforts we engaged in, we come to the following recommendations:

1. Invest in a more advanced process model for fire emissions in the CO_2MVS both for longer-term reanalyses and for operational shorter-term forecast/assimilation cycles. This model would consolidate the emerging capacity to link higher resolution FRP (e.g., VIIRS), moderate resolution burned area (e.g., Sentinel2), impact of small fires (e.g. GFED5), the simulated moisture state (IFS, ECland), and fuel loads as well as combustion completeness, in a dynamic real-time calculation of carbon emissions.
2. Use dynamic (i.e., weather-dependent) emission factors (EFs) to speciate the total carbon loss to CO_2, CO, NMHC, other gaseous species, and aerosols. This allows multi-tracer observations to validate the EFs, and to possibly constrain EFs as part of the data assimilation.
3. Use CO as pilot species in these attempts rather than NO_2, as the short NO_2 chemical lifetime and nonlinear decay close to the source complicates its interpretation even on scales of several kilometers, which for now remains at the edge of the capacity of a global CO_2MVS system.
4. Prioritize the building of a framework for the interpretation of CO satellite observation (XCO). Next to fire emissions and emission factors, focus on oxidation of shorter-lived species emitted from (rain)forests, as well as on emissions from savanna burning. These emissions co-locate with deforestation fires in many tropical countries and monitoring is required to deliver information on annual deforestation totals to stakeholders.
5. Support the development of QA/QC for an annual multiyear reanalysis of LULUCF emissions within the CO_2MVS. Leverage more extensive datasets not available in near real-time such as (a) atmospheric CO observations from NOAA, ICOS, GAW, etc, (b) other satellite datasets such as burned area, TROPOMI formaldehyde, but also upcoming biomass missions, and (c) estimates made with different bottom-up (bookkeeping) and top-down (other global data assimilation) systems.

2 Introduction

2.1 Background

The global CO_2 Monitoring Verification System (CO_2 MVS) of the Copernicus CO_2 Service is envisaged to not only make use of atmospheric CO_2 observations, but also from co-emitted species. This is needed to distinguish various sources of CO_2 to the atmosphere, each associated with different human activities. The combustion of fossil fuels is one prominent example, and a clear target for the CO_2MVS (Balsamo et al., 2021). Land-use, land-use change, and forestry (LULUCF) is a second, as its net carbon emissions contribute 1.3 ± 0.7 Gt C yr^{-1} (Friedlingstein et al., 2023) to the annual emissions of CO_2. This net impact is the result of emissions mostly from deforestation (1.9 Gt C yr^{-1}) and uptake of CO_2 by managed forests (-1.3 Gt C yr^{-1}), with carbon loss from peatland drainage and burning and wood harvesting contributing a smaller source (0.6 Gt C yr^{-1})

These numbers come with large uncertainty though, and considerable challenges remain in reconciling country-level LULUCF carbon balances reported to the UNFCCC, with those derived from bookkeeping models (Deng et al., 2022; Grassi et al., 2023; Obermeier et al., 2023; Schwingshackl et al., 2022). Observation-driven estimates mostly focus on direct carbon emissions from fires used in deforestation, and provide an additional view of land-use change fluxes. Each of these methods contributed to the first Global Carbon Stocktake (Byrne et al., 2023; McGrath et al., 2023), but their spread clearly demonstrates the need for a further integration of the data streams, and continuous verification of emissions in the Copernicus CO_2MVS. The need for improved LULUCF monitoring capacity becomes even more urgent with countries including negative emission strategies through reforestation in their plans to reach the goals of the Paris Agreement.

Fire emissions remain a primary target for inclusion in an MVS. Currently, their monitoring relies primarily on remote sensing such as fire radiative power (FRP), active fire detections (Giglio et al., 2016) and burned area (Giglio et al., 2018). Combined with biogeochemical information on standing carbon stocks, fuel loads, and combustion they allow fire emission models of various complexity, which are widely used (Kaiser et al., 2012; Werf et al., 2017; Wiedinmyer et al., 2011). They allow quick assessments of unusually intense fire seasons such as in Brazil in 2019 (P. M. Brando et al., 2020; Paulo Brando et al., 2020) attributed to increased deforestation (Gatti et al., 2023). But fires smaller than the conventional MODIS footprint (500m) -so called small fires- are hard to detect with burned area algorithms, yet can contribute substantially to carbon emissions Randerson et al (2012). This is also true for understory fires (Morton et al., 2013) which cause forest fragmentation, mortality, and higher vulnerability to subsequent burning (Alencar et al., 2006; Nepstad et al., 2001).

Additional to remote-sensing of the land-surface, atmospheric remote sensing was shown to provide constraints on total carbon lost from all fires across larger regions (Basso et al., 2023; S. Naus et al., 2022; Velde et al., 2021; Zhang et al., 2014). Column integral retrievals of CO (XCO) from MOPITT, IASI, and TropOMI show high signals relative to background CO from active fires, with both plumes and larger-scale XCO enhancement traceable to sources. This allows CO emissions to be optimized in a data assimilation framework, and to be converted into equivalent carbon emissions with assumptions on the emission ratio of CO to carbon. In various recent studies such as by (S. Naus et al., 2022), (Koren, 2020) but also (Peiro et al., 2022) and (Basso et al., 2023) a two-step approach was taken. First, a CO-only inversion was done to optimise fire emissions. Subsequently, these CO fire emissions were converted to CO_2 using predetermined emissions factors, and the resulting fire CO_2 emissions were used as a fixed fire emission in a CO_2-only inversion.

These studies concluded that combining fire emission models driven by surface remote-sensing, and atmospheric inversions driven by XCO, improved the estimated carbon lost from deforestation. The fire emission models, including GFASv1.2 currently in CAMS and the CO_2MVS, were found to be too low in their CO emissions, and require more carbon lost from

fires. We note though that in these studies, CO and CO_2 were not considered simultaneously, and the potentially large impact of the assumed emission ratios was acknowledged, but not addressed. Since then, new insights on higher resolution fuel consumption (Wees et al., 2022), dynamic emission factors (Vernooij et al., 2023), and the role of small fires in shaping burned area (Chen et al., 2023) suggest that substantial progress can be made on fire emissions modelling, with likely large impacts on derived CO and CO_2 budgets in a CO_2MVS. Especially the magnitude of savanna fires and their highly variable CO yield seems an important new consideration. With savanna grasses constituting mostly of C4 grasses, this signal might separate from deforestation (C3) in isotopic composition as well Randerson et al (2005). Together, this motivated the development of a multispecies data assimilation framework under CoCO$_2$.

Here we report on the progress that was made on multi-species (specifically CO) modelling and data assimilation using satellite observations (e.g. OCO-2, TROPOMI, MOPITT) for improved source attribution of land use, land use change, and forestry (LULUCF) emissions.

2.2 Scope of this deliverable

2.2.1 Objectives of this deliverable

This Deliverable documents a number of design choices for a CO_2MVS targeting deforestation emissions. It takes a specific view from the satellite monitoring perspective, and the use of CO as a proxy for total carbon emissions. We aim to advise on the use of a fire emission model, the approach towards emission factors and injection heights, and the simulation of the full CO_2 and CO budgets. We separate their role in 10-day operational MVS and in multi-year reanalyses.

2.3 Work performed in this deliverable

For this Deliverable we built a forward modelling system with fully coupled CO/CO_2 budgets, already integrated into the CarbonTracker Data Assimilation System (CTDAS) to allow ensemble Kalman smoothing in a follow-up project. We equipped our model with four different fire emission models, two different approaches for injecting fire plumes into the atmosphere, and employ both static and dynamic emission factors. A full evaluation of simulated CO and CO_2 was enabled through the sampling of XCO from MOPITT v9, TCCON profiles, aircraft flasks (Luciana Gatti Amazon network), surface flasks (NOAA), and in-situ time series (ATTO). We present simulations in various configurations and come to recommendations on the strategy to follow for development of the CO_2MVS.

2.3.1 Deviations and counter measures

(1) The original proposal mentioned NO_2 from TropOMI as a possible tracer to assess fire emissions. Based on work in WP4, and in a separate project (SENSE4FIRES, V. Huijnen personal communication), we concluded that the NOx chemistry is too fast at the scale of global transport models (10-100km). This means that local plumes from combustion sources are not conserved in shape and composition, and moreover that the chemical lifetime of NO_2, an important property to model correctly for interpretation of XNO2, cannot be simulated in a realistic way (Lorente et al., 2019). We therefore decided not to focus our TM5 efforts on this tracer, until a viable and fast parameterization of the nonlinear chemistry is built.

(2) Although our multi-tracer DA framework is ready and operational for CO_2 and $d^{13}C$, it is not yet tested for CO. This means we have not yet assessed the influence of window lengths in DA, or the optimization of a statevector and background covariance matrix that includes emissions as well as emission ratios. These simulations will start in January 2024 and will be completed under the umbrella of two follow-up projects with Copernicus involved (CORSO and CATRINE).

(3) We focused our simulations on the year 2019 instead of 2021, because the Amazonian fires presented a better case to evaluate and test the system. The burning of tropical forest should yield a substantial amount of carbon to the atmosphere that should be well-detectable in observations (e.g. from space). Also, both tropical forest and savannah burned, which is interesting from the perspective of emission ratios. Finally, we had a unique set of observations for 2019 available. In consultation with ECMWF we will decide which year to focus our multi-year DA efforts on.

(4) We note that TropOMI data was sampled in the runs presented in this Deliverable, but the smaller data volume of MOPITT allowed faster assessment and less computational overhead. We thus present these results, after verifying that the comparison with the higher resolution TropOMI data does not alter our conclusions. If our work leads to a publication we will prioritize the TropOMI data.

3 Modelling framework:

3.1 Description

The CarbonTracker Data Assimilation System (CTDAS) includes CarbonTracker Europe and South America, which form the foundation of the system presented here (Laan-Luijkx et al., 2017; Peters et al., 2007; Velde et al., 2018). We further build on this system by integrating the CO budget, based on the work by Naus et al., (2022), which is also based on the TM5 model, but uses long-window 4D-VAR emission optimization. CTDAS consists of several components that bring together observations (in-situ and satellite), a global transport model, and an ensemble Kalman smoother, in one python-based shell. It allows a forward modelling system to be built and evaluated while re-using components from existing codes, or adding custom capacities. Once the forward framework works satisfactorily, optimization of a flexible statevector is relatively straightforward to add, hence our choice for this approach. Developments under this Deliverable have fully completed the CTDAS forward framework for CO and CO_2 including evaluation presented here, while the data assimilation component is in progress.

We calculate atmospheric transport of CO_2 and CO with the Tracer Model 5 Massive Parallel (TM5-MP, see also Huijnen et al., 2010 and Krol et al., 2001). Transport is driven by ECMWF reanalysis data, ERA5 (Hersbach et al., 2020). In the TM5-MP CO/CO_2 system the CO and CO_2 budgets are coupled. This coupling takes place through the main loss term of CO, which is oxidation by the hydroxyl radical (OH), producing CO_2. The lifetime of CO against OH-removal is 2-4 weeks. This is included in our system based on pre-calculated OH-fields from a previous TM5-MP simulation by Myriokefalitakis et al., (2020) that used full-chemistry (also of CO and OH) and that was evaluated to have realistic OH-distributions. Chemical production of CO from NMHC and CH_4 oxidation is also not calculated online but also taken from Myriokefalitakis et al. (2020). This allows a relatively cheap simulation of the coupled CO and CO_2 budgets without the need for expensive full-chemistry simulations. CO loss by dry deposition is calculated online based on Ganzeveld et al., (2002). Table 1 contains an overview of the surface and 3D input fields and initial conditions of the system.

The simulations presented in this report were conducted at 3°x2° global grid and on 34 vertical levels.

Table 1: TM5-MP/COCO$_2$ setup

Configuration	
Meteorological forcing	ERA5 (Hersbach et al., 2018)

CO_2 priors (following CTE v2023)	
Fires	GFASv1.2 : (Giuseppe et al., 2018; Kaiser et al., 2012; Rémy et al., 2017)
Biosphere	SiB4: (K D Haynes et al., 2019; Katherine D Haynes et al., 2019)
Fossil fuels	GridFEDv2023.1: (Jones et al., 2021)
Ocean	Carboscope v2022 (Rödenbeck et al., 2013)
CO priors	
Fires	GFASv1.2 : (Giuseppe et al., 2018; Kaiser et al., 2012; Rémy et al., 2017)
Fossil fuels	MACCity: (Granier et al., 2011)
Chemical production from CH_4	TM5-MP full-chemistry run (Myriokefalitakis et al. 2020)
Chemical production from NMVOCs	
Initial conditions	
CO_2 fields	CTE(v2023) run for the Global Carbon Project (Friedlingstein et al., 2023)
CO fields	CAMS EAC4: (Inness et al., 2019)
OH fields	TM5-MP full-chemistry run (Myriokefalitakis et al. 2020)

3.2 System evaluation

This Section includes a brief validation of a 2-month run (27/07/19 - 30-09-19). In this “base run” all emissions are injected at the surface and GFAS v1.2 is used as fire model.

The bar plots presented in Fig. 1 show a comparison of CO_2 and CO mole fractions against a subset of NOAA background stations. For CO_2 we get close to the observations (deviations 0.3±0.6 ppm) as expected since we start from an optimised CarbonTracker Europe field. CO is structurally overestimated with 9±5 ppb. This overestimation follows a known north-south gradient, consistent with findings by Myriokefalitakis et al. (2020). The magnitudes of these biases align with non-optimized results reported by Naus et al., (2022) and partly relate to incomplete bottom-up knowledge on the CO budget, and possibly to inaccurate OH-oxidation fields (Naus et al 2021; Rigby et al 2017)

Comparisons with OCO-2 LNLG (v11) column average dry air CO_2 amount fractions (X_{CO_2}; Fig. 2) reveal a mean bias of 0.3±3.1 ppm with weak signs of latitudinal dependence. Compared to TCCON data (Fig. 3), we find a comparable mean bias of 0.5±2.0 ppm. Further assessment against MOPITT V9 TIR X_{CO} retrievals (over land) in Figure 4 indicate a mean bias of -16±22 ppb, which is in line with the surface observations and Naus et al. (2022).

Overall, these results provide us with confidence in the model's performance. Nevertheless, they also show there is room for improvement and underline the opportunity and need for additional constraints from atmospheric observations. In the next sections, we dive into the modelling of fire emissions.

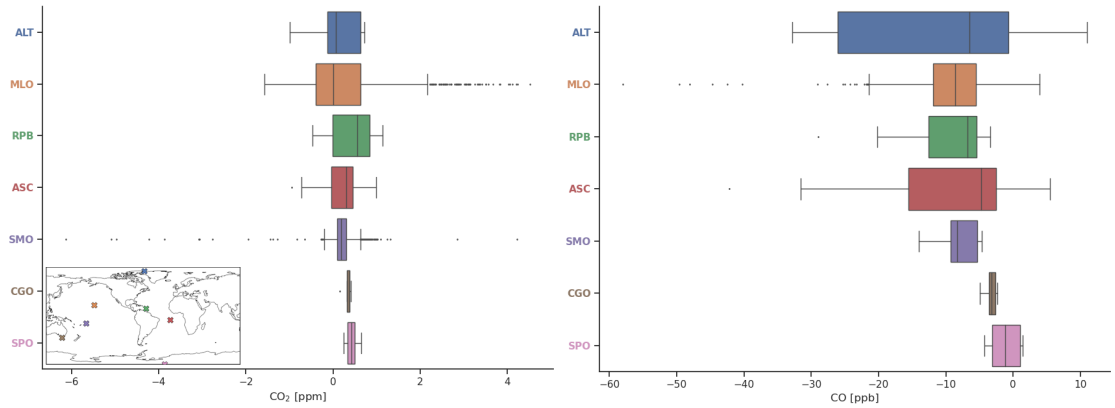

Figure 1: Boxplots with CO_2 (left) and CO (right) residuals (ppm and ppb obs-minus-model) at NOAA background stations: Alert (ALT), Mauna Loa (MLO), Ragged Point (RPB), Ascension (ASC), Samoa (SMO), Cape Grim (CGO), South Pole (SPO). Simulations with TM5 @ glb300x200, Aug-Sep 2019. The figure shows small CO_2 residuals as expected for an optimized budget, and a CO overestimate by the model as reported in other studies using the same unoptimized set of CO emissions and production terms.

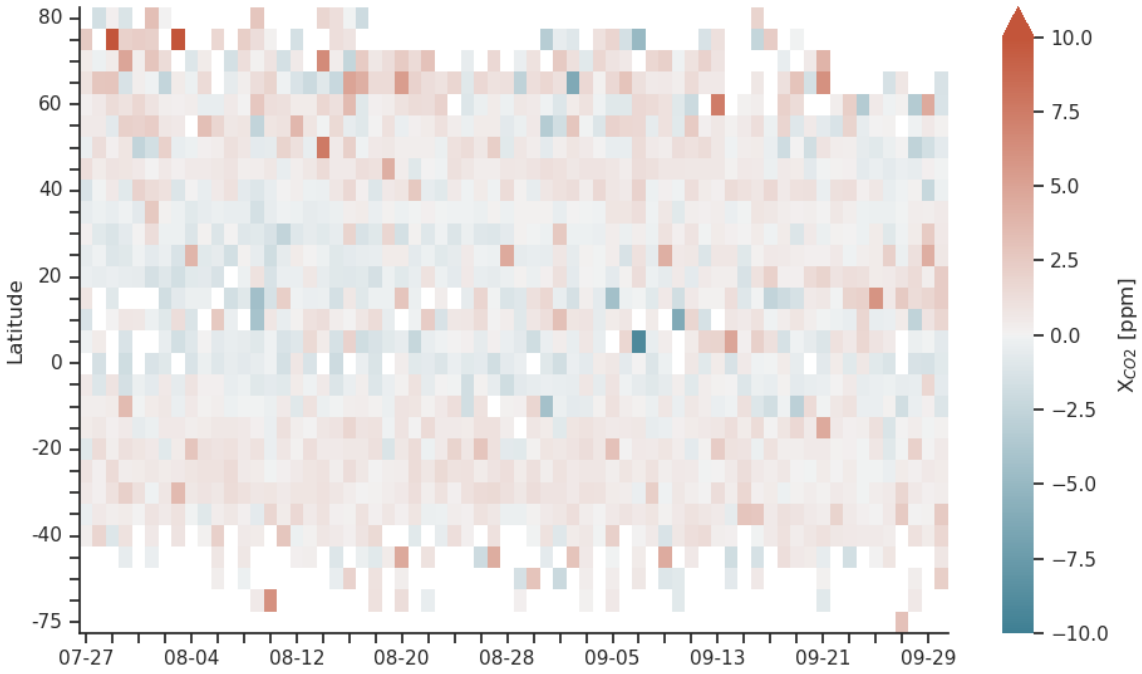

Figure 2: X_{CO_2} residuals compared to the OCO-2 L2 Lite v11r product averaged over 5°x360°x1day bins. Observations processed to 10s averages (Crowell et al., 2019), only including land nadir/land glint soundings (LNLG). Small XCO_2 biases show consistency between the surface-based optimization and independent satellite data, but also possibly latitudinal differences.

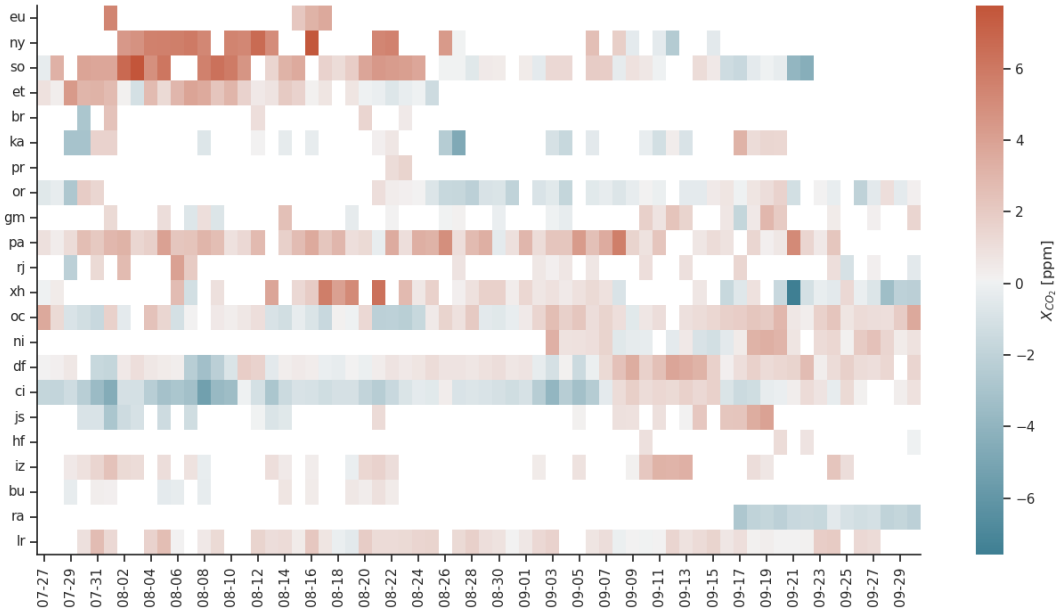

Figure 3: Daily average X_{CO_2} residuals compared to TCCON stations (GGG2020), y-axis sorted on latitude.

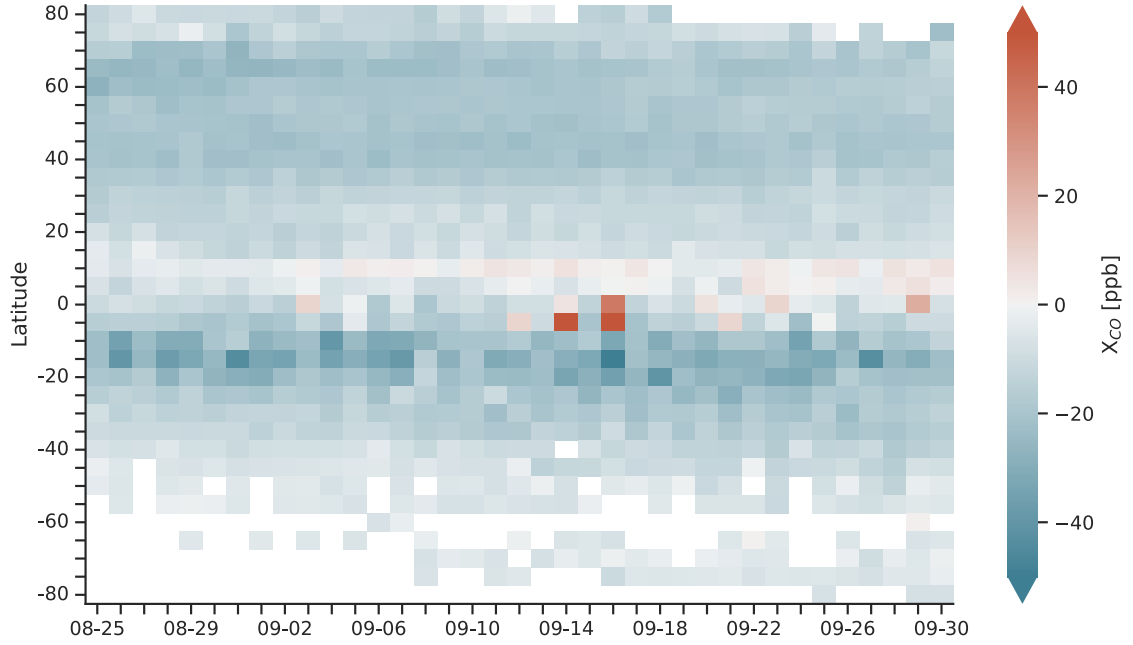

Figure 4: X_{CO} residuals compared to the MOPITT V9 TIR product averaged over 5°x360°x1day bins. The consistent model overestimate of XCO in blue colors stems from a known overestimate of CO given the unoptimized budget we prescribe. Positive deviations in the tropics likely stem from (unoptimized) biomass burning.

4 Sensitivity analyses and recommendations

This Section presents a series of sensitivity experiments to illustrate the importance of several prior and model-design decisions in the context of a satellite driven joint CO-CO$_2$ inversion setup.

The simulations referred to in this section were conducted globally, but this Section specifically pays attention to the late dry season over Amazonia in 2019. During this period, there was a surge in fire-activity. The co-existence of both tropical forest and savanna ecosystem fires in this region and during this timeframe presented a good opportunity to better quantify the role of different emission ratios. Moreover, we had access to a unique set of observations from satellites (OCO-2, MOPITT) as well as in-situ (aircraft profiles and tower). Together, these presented a good opportunity to test the TM5-MP/COCO$_2$ setup and impact of fire related modelling choices. Our interpretation mostly focuses on XCO and XCO$_2$ columns, as these will likely form the main data constraints on LULUCF emissions in a future CO$_2$MVS.

4.1 Fire priors and role of small fires

We first investigate the impact of different fire prior emission datasets on simulated CO and CO$_2$. This was done in previous publications too, mostly to conclude that differences are substantial and that observational constraints can agree with different products at different times and locations. Generally, tropical South American fire emissions in GFAS and GFED4 were found to be too low during previous large fire events, while FINN tends towards higher emissions (Naus et al., 2022).

We ran simulations with these three emission inventories, and we included a beta version of the new GFED5 product (Chen et al., 2023). The latter takes advantage of higher resolution data to capture the substantial impact of small fires, and uses updated (weather dynamic) emission factors for savannah burning. Fire emissions for these simulations were injected with IS4FIRES day/night profiles for maximum realism in assessing the impact. The main characteristics of the four sets of fire emissions are:

- **GFAS v1.2** is included in the CAMS forecasts and is based on near real-time retrievals of FRP from MODIS Terra and Aqua. Daily emission files are available since 1/1/2003 on 0.1 degrees global resolution, and cover total carbon as well as its speciation (CO, NOx, ..). Emission Factors for this speciation are however static and are based on Andreae & Merlet (2001) data. Injection height daily data is provided by a plume rise model and IS4FIRES.
- **GFED4S** is based on burned area from MODIS (Collection 5.1) and fuel consumption based on the Carnegie Ames Stanford Approach model (Van der Werf et al., 2017). It supersedes GFED3 which was used to constrain FRP to carbon emission ratios in GFAS. It covers the 1997 to the present time period and is available on a 0.25 degree global grid using emission factors mostly from Akagi et al., (2011). Its temporal resolution is monthly but active fire detections are used to move from monthly to daily (2-daily in the tropics).
- **GFED5 (beta)** builds on GFED4s but its small fire algorithm is now constrained by moderate resolution burned area datasets (S2, Landsat) for selected regions (Chen et al., 2023) which roughly leads to a doubling of global burned area compared to MODIS collection 6 data (Giglio et al., 2018). Fuel consumption is based on a simplified version of the CASA model (Van Wees et al., 2022) running at 500m. Due to the statistical nature of the small fire algorithm both datasets are merged to 0.25 degree spatial resolution with biome-level burned area within that grid cell multiplied by biome-level fuel consumption. The conversion from a monthly to a daily timestep is similar to that used in GFED4s.

- **FINN v2.5** uses active fire detections from MODIS and VIIRS to calculate emissions at 1x1 km resolution. Active fire detections are converted to burned area using biome-level scalars and fuel consumption is derived from van Leeuwen et al., (2014) and is thus solely biome-dependent. Global total carbon emissions from FINN2.5 are substantially higher than previous versions (Wiedinmyer et al., 2023).

A substantial difference in XCO stems from the choice of fire model, which makes it likely that XCO retrievals can improve our knowledge of deforestation emissions. Consistent with Fig. 4, the boxplots in Fig. 5 show differences of up to 10 ppb in XCO residuals against MOPITT land-only data points globally, in not just their spread, but also their means. Importantly, the total residuals shown have spatial and temporal structure, due to the underlying differences in emissions.

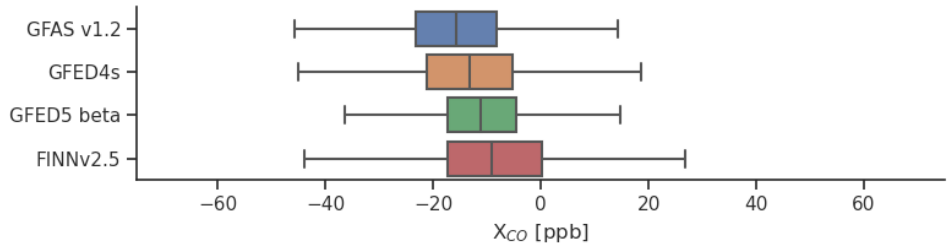

Figure 5: X_{CO} residuals (obs-minus-model) for simulations with different fire priors compared to MOPITT V9 TIR retrievals over land (global) between 25/08 and 30/09.

Interestingly, fire emissions at first glance appear quite similar in spatial patterns owing to a large similarity in the underlying satellite observations of FRP, active fires, or burned area. But the absolute and relative intensity of the CO emissions vary, as shown in Fig. 6. This suggests that data assimilation of XCO will mostly be useful to constrain the emission intensity across time, and across different burning regions. In addition, the total fire CO emissions (and by inference also carbon emissions) will be a target for optimization, as the totals from e.g., FINNv2.5 are much larger than from GFASv1.2 over the period shown.

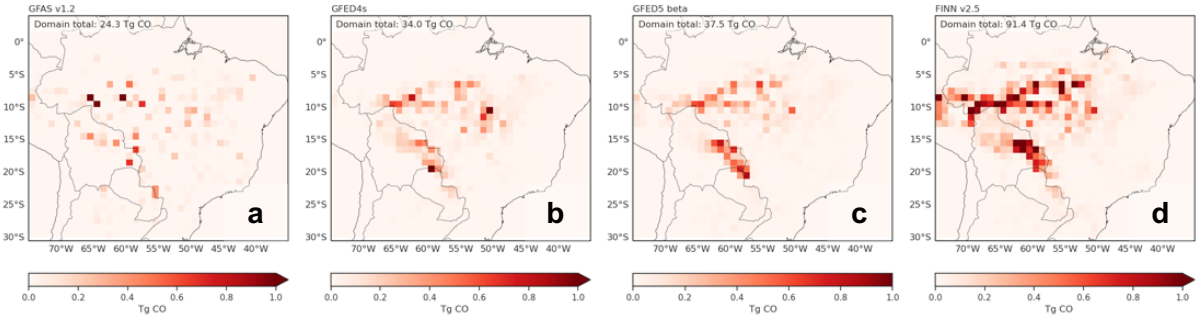

Figure 6: Fire CO emissions over Amazonia between 27/07 and 30/09 per 1°x1° gridbox in each of the tested fire inventories: (a) GFAS v1.2, (b) GFED4.1s, (c) GFED5 beta, and (d) FINN v.2.5.

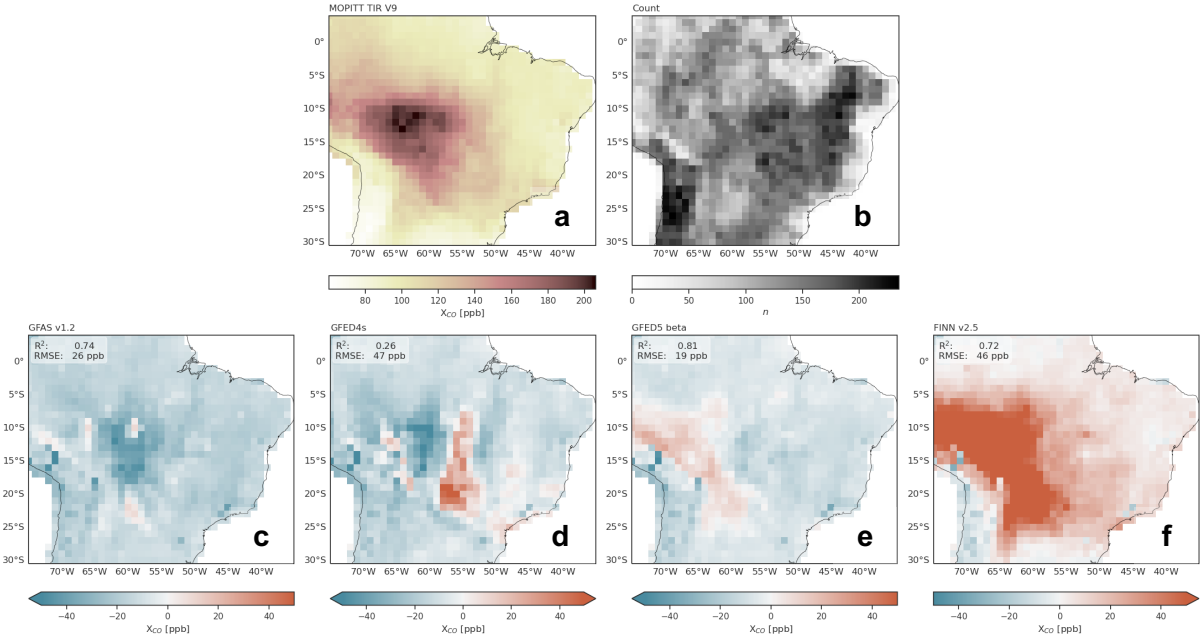

Figure 7: (a) Mean X_{CO} columns over Amazonia between 25/08 and 30/09 from MOPITT TIR v9 and respective (b) number of observations per 1°x1° bin. The subsequent panels show X_{CO} residuals (note: model-minus-obs here) for simulations with (c) GFAS v1.2, (d) GFED4.1s, (e) GFED5 beta, and (f) FINNv2.5 as fire emission model.

The large range of emissions shown in Figure 6 also lead to strongly contrasting XCO patterns in the atmosphere over Amazonia. Figure 7 shows the residual of XCO over Amazonia averaged over 5 weeks during the 2019 dry season for each of the fire emission models, given the same transport with the TM5 model. The FINNv2.5 modeled columns (panel f) are too high by several 10's of ppbs over the full domain, clearly separating them from the GFED4s (panel d) simulations which rather show a dipole of too high columns in the eastern Amazon and too low columns in the central Amazon. GFASv1.2 is generally too low compared to MOPITT in these months, fully consistent with earlier findings (see Figure 5 of Naus et al., 2022). GFED5 beta has smallest mean residuals and the highest spatial correlation coefficient (R^2=0.81) of the set. This suggests that its incorporation of small fires (Chen et al., 2023) and updated emission factors for savanna burning (Vernooij et al., 2023) relative to GFED4s could be a strong driver of more realistic CO fire emissions. Future analyses will investigate the role of small fires, here we further investigate the role of the emission factors.

Recommendation: Invest in building the best possible deforestation + fire emissions model to provide a starting point for atmospheric data assimilation. This model should include the influence of small fires and use high-resolution FRP, or active fires in operational mode, and burned area in reanalysis mode. Machine-learning can link FRP or active fires to emissions from this model, allowing a fast transfer of information.

4.2 Emission Factors

When using XCO as observations in the CO$_2$MVS, the conversion of total CO emissions to carbon release (our target variable) will crucially hinge on the Emission Factors (EFs) used to partition the fuel consumed (in kgC) into various species. When interpreted as resulting ratios of tracers in the atmosphere these are also referred to as emission ratios (ERs). Traditionally, different ERs have been associated with different land-use types and fire types and later on (Andreae & Merlet, 2001) also with different fuel wetness which is a function of recent weather (Leeuwen et al., 2013; Vernooij et al., 2023). ERs can thus vary over space and time and influence observed XCO and XCO$_2$.

Figure 8 shows the ERs associated with fires in GFAS and GFED5 over our study domain and period. While overall patterns are similar at first sight due to the underlying land-use types,

closer inspection shows (a) many more fires with low ERs in GFED5 due to the detection of small fires mostly in non-forest landscapes, and (b) high ERs typical of moist forest (>80 ppb/ppm) are flanked by low ERs typical of low vegetation (<60 ppb/ppm) in deforestation areas in the central Amazon, lowering mean ERs in the coarsened 0.25°x0.25° map of GFED5. Moreover, GFED5 ERs have a standard deviation that can be as large as ±15 ppb/ppm as they vary over time due to moisture conditions and other parameters changing for savanna fires.

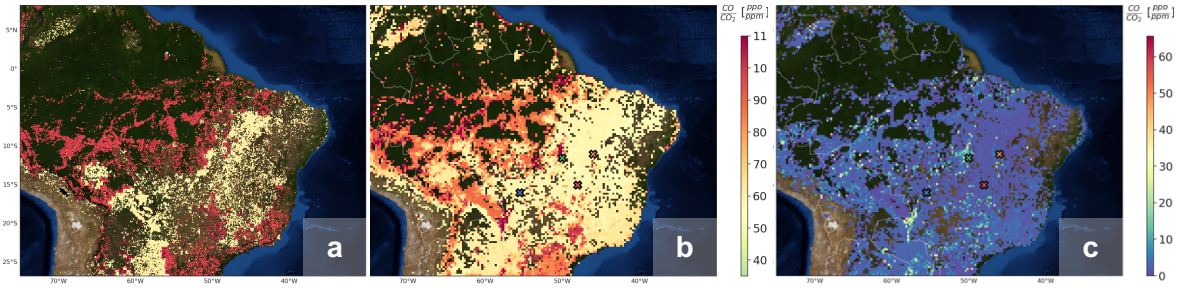

Figure 8: CO/CO$_2$ emission ratios (ERs) for fires that occurred between 27/07 and 31/09 in (a) GFASv1.2 and (b) GFED 5 beta on their native resolutions (0.1°x0.1° and 0.25°x0.25° respectively). Panel (c) shows the standard deviation for (b). The crosses in panel (b) and (c) indicate the locations of time-varying ratios plotted in Fig. 9.

These temporal variations are further detailed in Fig. 9, which shows the ER timeseries over four locations marker in Fig 8c, each classified as savannah. For reference, the constant ER used in GFASv1.2 (58 ppb/ppm) for all savanna fires is shown as a horizontal line. Clearly, variations in ER matter. For example in the blue boxes corresponding to the southernmost location, the ERs increase by nearly 10% in a few weeks' time. When minimizing the difference between observed and simulated XCO, not accounting for the ER increase would require 10% higher carbon emissions in the latter part of the month instead. Similarly, a systematic deviation from the fixed ER would bias carbon emission estimates proportionally, as the ER (or EF if referring to emissions) is a multiplicative term between carbon lost and CO emitted.

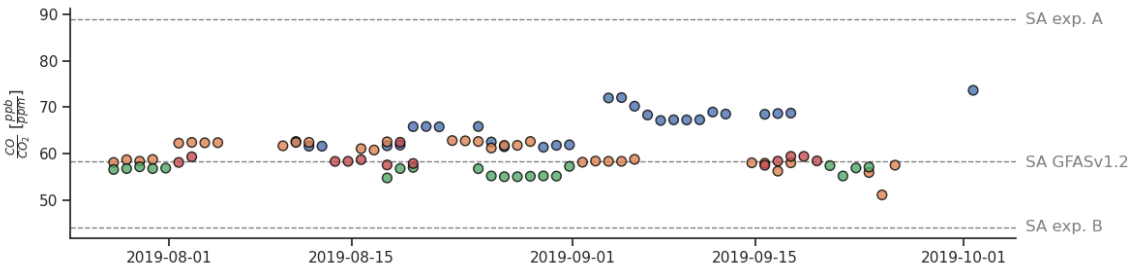

Figure 9: GFED5 beta CO/CO$_2$ emission ratio timeseries for gridboxes classified as savanna (11.5°S, 50.0°W; green), (11.0°S, 46.0°W; orange), (16.0°S, 55.5°W; blue), and (15.0°S, 48.0°W; red). The middle horizontal grey dashed lines represent the currently implemented fixed ERs for savanna burning in GFASv1.2 (SA GFASv1.2) according to Kaiser et al. (2012). The upper (SA exp. A) and lower (SA exp. B) dashed lines are the ERs used in the sensitivity experiment presented in Figure 10.

Errors in EFs on the fire emissions propagate through the atmosphere and can have non-local effects that may bias carbon emission estimates downwind of the regions. To illustrate this, we conducted an experiment in which the ERs for savanna (SA) and tropical forest (TF) fires were changed to the respective low/high end of their literature estimate as in Table 2. Total emitted carbon was kept constant.

Table 2: Description of emission ratio sensitivity experiments.

Experiments		
	Experiment **A**	Experiment **B**
ER_{SA}	Low	High
ER_{TF}	High	Low
CO/CO_2 emission ratios [ppb/ppm]:		
	ER_{SA}	ER_{TF}
Default: GFAS v1.2 (Andreae & Merlet; 2001)	58	98
Low	44	60
High	89	145

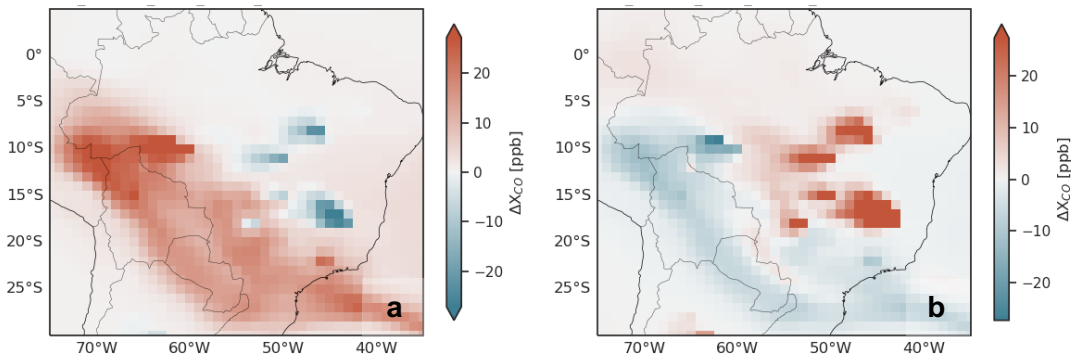

Figure 10: Change in X_{CO} columns for simulations with adjusted emission factors compared to the default. Scenario A: ER_{SA} low, ER_{TF} high (a), Scenario B: ER_{SA} high, ER_{TF} down (b).

The difference in XCO between the default and experiment A (low SA/high TF) and B (high SA/low TF) is illustrated in Fig. 10 above. Over large areas of the domain the colours are inverted, as the savanna fires in the north-eastern part of the domain emit less or more CO than the default, and the tropical forest vice versa. But on the savanna/forest borders (e.g., 15°S 55°W) both experiments show higher columns than the default, with a red plume extending to the south of the domain. This 'mixed' zone moves with the synoptic flow and signifies the region where XCO is likely to be sensitive specifically to regional ER differences.

Recommendation: Move towards a fire model with dynamic (i.e., weather-dependent) emission factors (EFs) to speciate the total carbon loss to CO_2, CO, NMHC, other gaseous species, and aerosols. Develop capacity to vary or constrain EFs as part of the data assimilation for fire carbon emissions. Machine-learning of EF variability can provide a fast estimate to use in operational CO_2MVS and should be pursued.

4.3 Injection heights

In this section, we test the sensitivity of simulated XCO for injection heights. It is well established that injection heights play a key role in the subsequent transport of the emitted gases and aerosol (Kahn et al., 2008; M. Krol et al., 2013; Martin et al., 2010; Rémy et al., 2017; Sofiev et al., 2012, 2013). Plume rise of biomass burning plumes is determined by FRP, but also by the atmospheric stability and moisture content (Freitas et al., 2009; Virgilio et al., 2019).

We tested the impact of different emissions heights in the comparison between simulated XCO and the MOPITT V9 TIR product. Three cases were considered: Scenario “Surface” emitted all biomass burning at the surface, scenario “IS4FIRES whole day” used a single emission profile per day from IS4FIRES (Sofiev et al., 2012), and scenario “IS4FIRES day/night” employed different emission profiles for day and night. Figure 11 shows that the impact on the residuals is minor, the reason being that columns are being compared. Obviously, the secondary effect of the different transport pathways associated with the different main emission altitudes plays only a small role.

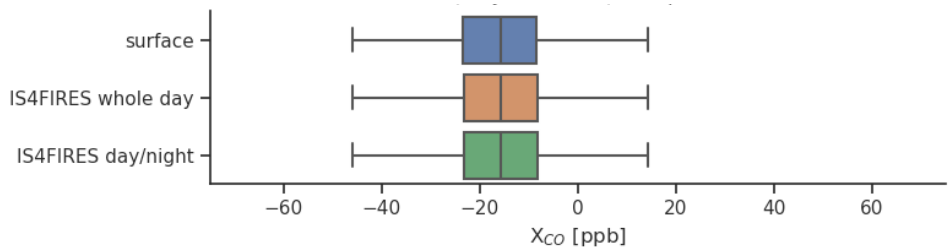

Figure 11: X_{CO} residuals for simulations with different injection heights compared to MOPITT V9 TIR retrievals over land (global) between 25/08 and 30/09.

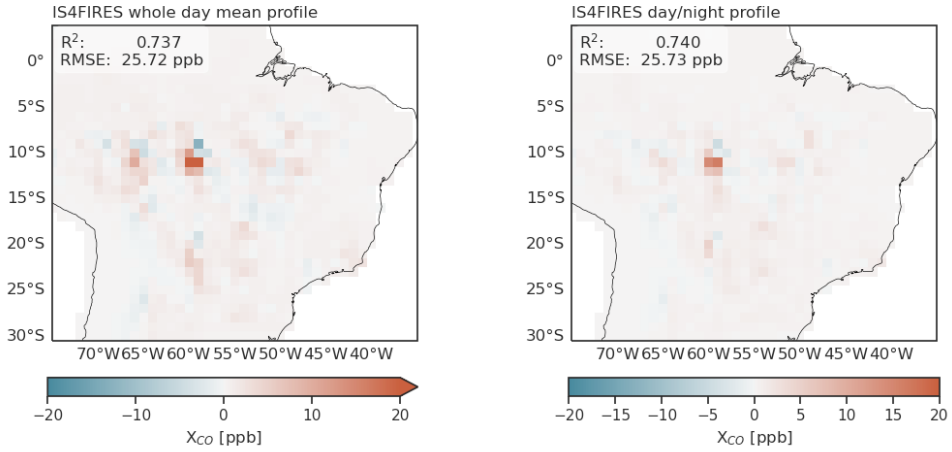

Figure 12: Spatial difference in X_{CO} over Amazonia for simulations with injection profiles compared to emissions injected at the surface. R^2 and RMSE show the performance of each run compared to MOPITT V9 TIR.

This is further illustrated in Fig. 12, which shows the spatial impact of emitting biomass burning emissions using different profiles. The figure shows differences in the XCO column with respect to the simulation that emits at the surface. Locally, differences can still be up to 20 ppb in the column, but mean statistics with respect to MOPITT hardly change.

As expected, differences are larger at specific altitudes or when profiles are compared, specifically near large emissions. Fig. 13 displays a comparison of CO enhancements with results from an airplane-derived profile near Tefe (Amazonas state), a site that if often influence by biomass burning plumes. The CO enhancements shown in the figure were calculated by subtracting a background based on Ragged Point, Barbados. This is one of the available observations for which a clear biomass burning signal was present.

The calculated enhancements in the model have the correct profile shape, but the profiles are less steep compared to the aircraft observations. For this specific case, differences of almost 10 ppb are found between the simulations, but the simulated profiles have similar shapes. Thus, the profile shape is governed by transport processes that occurred after emission. Moreover, differences with the observations are larger than between the different simulations, likely due to the local characteristics of the observations. Note that the model resolution is roughly 100 km.

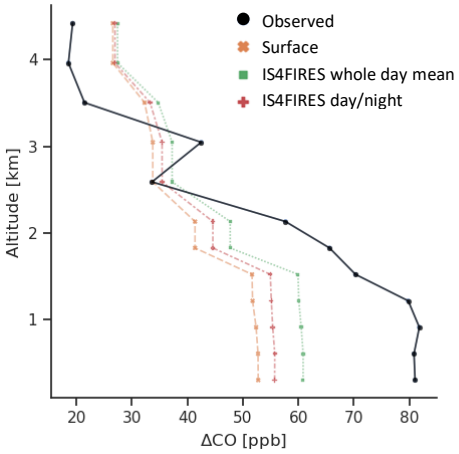

Figure 13: Comparison of CO enhancements from simulations with different injection heights to a vertical profile near Tefe, Brazil. CO observations courtesy of Luciana Gatti, Lagee lab, INPE, Brazil.

From this sensitivity simulations we conclude that profiles that are used to distribute biomass burning in the vertical are not a critical factor when comparing to satellite XCO columns from MOPITT TIR products. Part of this low sensitivity might be due to the limited sensitivity of MOPITT TIR to surface CO, and the fact that the model profiles are convolved with the averaging kernel when they are compared to MOPITT. The sensitivity might be larger with the TROPOMI XCO, which has higher sensitivity to surface CO (Leguijt et al., 2023).

Likely, the current implementation in GFAS (Rémy et al., 2017) provides a reasonable estimate for the vertical distribution of biomass burning emissions. Further optimization of these profiles, e.g. by adding the emission profile in the state vector, is therefore not recommended.

Recommendation: Simulated XCO shows low sensitivity to the vertical emission distribution, so improving injection heights and biomass burning emissions profiles should not be given high priority when the aim is constraining continental-scale carbon cycle dynamics.

4.4 NMHCs

Chemical CO production from CH_4 and NMHC oxidation is an important source term in the CO budget (~50-60%; e.g. (Bo Zheng et al., 2019)). Globally, roughly a quarter of this contribution is related to oxidation of short-living NMHCs. However, over densely vegetated regions such as Amazonia, the role of this secondary CO source becomes more important. NMHC oxidation, mainly from isoprene and terpenes, has a strong seasonality, related to (drought-) stress conditions. These are likely to occur in advance of – or during – fire-periods. In addition, combustion of biomass also releases NMHCs, which means NMHC oxidation CO is spatio-temporally correlated with fires. This implies that care is needed when observed CO enhancements are used to infer CO and CO_2 emission from fires.

An intermediate in the oxidation chain from Volatile Organic Compounds (VOCs) to CO is formaldehyde (CH_2O), which is observed by satellite instruments (Smedt et al., 2021; Zhu et al., 2016), albeit with small signals.

We quantify the contribution of secondary CO production over South America, an area with large emissions of NMHCs, but low contributions from industrial emissions. We calculated XCO enhancements compared to a mean background column over Patagonia. Fig. 14, shows that total X_{CO} enhancements are indeed not only determined by fires (Fig. 14c), but that there is a significant contribution from the CO production term (Fig. 14b; CH_4 and NMHC oxidation).

Averaged over the domain, this oxidation term by far has the strongest contribution to the total columns and cannot be ignored.

Thus, there is a substantial risk to misinterpret the CO from NMVOC oxidation as direct CO emissions from biomass burning. A LULUCF component of a CO$_2$MVS that exploits XCO products to estimate biomass CO$_2$ emission, should therefore account for this important term.

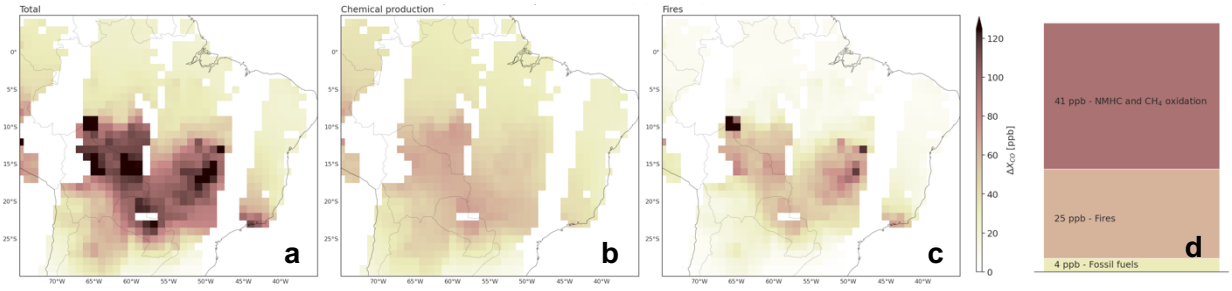

Figure 14: (a) Total X_{CO} enhancements during MOPITT V9 overpasses over Amazonia between 20/09 and 23/09 and contributions from (b) NMHCs and (c) fires. The stacked column (d) shows the domain and time average CO budget component contributions.

As seen in figure 14, the NMVOC-CO contribution is relatively smooth compared to the contribution from biomass burning. This could provide a way to separate the two contributions. Other ways to obtain information about the NMHC-CO production are:

- Full chemistry simulations that account for the emissions and chemical fate of VOCs could provide an estimate. In fact, we used such an estimate in our simulations. However, both VOC emissions and the subsequent chemistry are highly uncertain. These uncertainties are amplified by the tight coupling between VOC abundance and OH, the main sink for CO (Ringsdorf et al., 2023).
- Satellite observations of isoprene (Wells et al., 2020) and formaldehyde (De Smedt et al., 2021; Zhu et al., 2016) might provide constraints on secondary CO production.
- Isotopic information of CO can be used to infer the contribution of secondary CO production (Dasari et al., 2021; Vimont et al., 2019).

These methods are an area of active research, and an optimal strategy is currently hard to define. A multi-species inversion system (B Zheng et al., 2019), assimilating satellite information from the coupled atmospheric species CO, CH_4, and CH_2O, likely provides a good starting point.

We focused here on the Amazon, and the situation is likely quite different for boreal fires or Asian peat fires. Given the important contribution of LULUCF emissions, further research in this field is certainly needed. CO satellite products offer the best potential to constrain LULUCF emissions, mostly because their long heritage and the suitable lifetime of CO that leaves clear imprints of biomass burning in the atmosphere. However, uncertainties from secondary production of CO in the atmosphere should be dealt with in an appropriate way.

Recommendation: Explore methods to efficiently model and constrain the role of secondary CO production from NMHC oxidation.

4.5 Budget coupling: CO$_2$ production from CO

The CO$_2$ and CO budgets share fossil fuels and biomass burning combustion as source terms. In a CO$_2$ only version, CO$_2$ is generally counted as total carbon and thus absorbs the fraction emitted as CO or NMHC, assuming it is converted to CO$_2$ within several weeks. In our system we instead speciate carbon to both CO$_2$ and CO and let the conversion to CO$_2$ occur as a

function of the OH abundance in the atmosphere. Figure 15 quantifies what we call the “direct” effect of the coupling, which is that less CO_2 is released at the surface (and more CO, not shown). The figure illustrates the amount of CO_2 (in ppm) near the surface that is not emitted and thus not part of a model-observation comparison for CO_2. Although this is a small fraction of total carbon, locally this can be a several ppm difference at the surface, which is large enough to matter when interpreting local surface CO_2 observations. This is especially true for fires and thus for land-use change monitoring with surface observations.

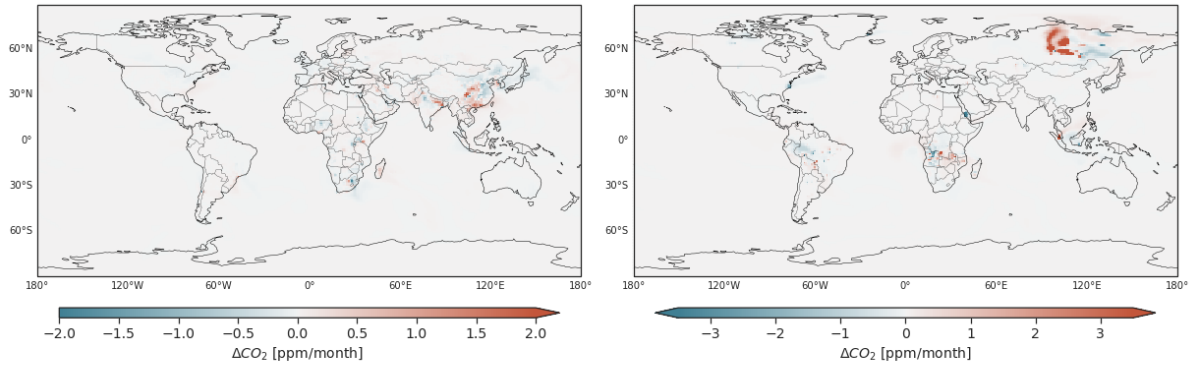

Figure 15: The "direct" impact of budget coupling for fossil fuels (left) and fires (right). The fields show amount fractions of CO_2 near the surface that would be emitted as CO_2, but now are “moved to CO”.

After this carbon is emitted as CO, it is transported away from the source and oxidised to produce CO_2, which we see as the “secondary” effect. The amount of CO_2 produced from CO, in column space is presented in Fig 16 for a simulation of one week. It shows small impacts that would be beyond the capacity to distinguish in observed XCO_2. Of course, this CO-derived CO_2 will accumulate over time but at the same time disperse and only add to the background gradients of CO_2, as illustrated for example in (Suntharalingam et al., 2005). At that time a large-scale inversion such as foreseen in reanalysis mode would show minor sensitivity to this coupling, while a short-term inversion as foreseen in operational mode would not be sensitive to the induced gradients.

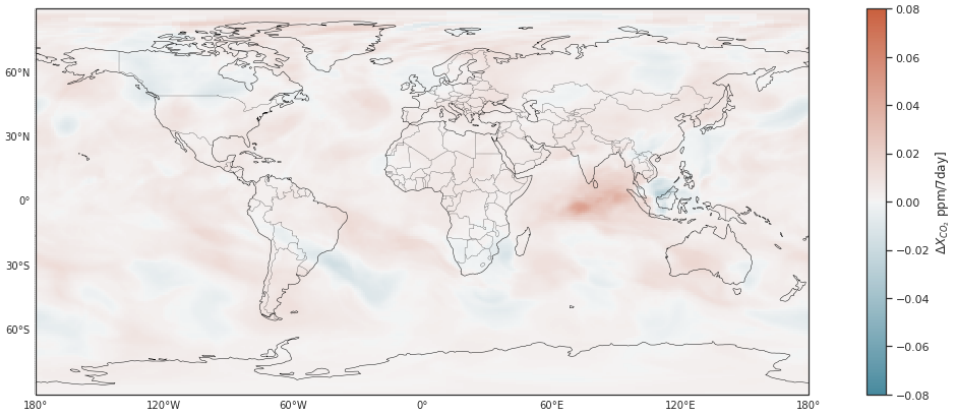

Figure 16: Change in X_{CO_2} related to CO_2 production from CO oxidation over 7days from (last week of run 21st - 28th September).

Recommendation: The budget coupling of CO_2 and CO matters more to emissions and surface CO_2 abundances than to XCO_2. The CO_2 production from CO should be considered explicitly mostly in the reanalysis mode when large-scale gradients are of concern to derive continental-scale emissions. Otherwise, the “direct” effect on emissions is most important for LULUCF monitoring.

5 Future outlook and recommendations

In this section we discuss the main recommendations that ensued from our work under $CoCO_2$. These are focussed on the goal to verify anthropogenic greenhouse gas emissions with Copernicus' CO_2-MVS system, with a specific focus towards emissions resulting from land-use change and forestry, as well as from fires. In many tropical countries these are highly connected through the use of fires in the deforestation process. In other regions of the world fires can be part of the natural landscape, or also caused by humans and hence tracing biomass burning emissions in the CO_2-MVS will be an indispensable part of simulating the full carbon cycle. This also means that inherent uncertainty in modelling biomass burning emissions, plume dispersion, and chemical transformations needs a place in the CO_2-MVS design.

An important recommendation resulting from our work is therefore to invest time and resources in building a state-of-the-art biomass burning model. There are two tracks of development for this:

(1) is the further development (beyond the current GFAS1.2 system) of a near real-time fire emission modelling capacity that depends only on a combination of Fire Radiative Power (such as directly available from VIIRS) and NWP variables from IFS. Such a model could be based on machine-learning of available FRP against historical emissions of GFED5, leveraging the integrating power of FRP over burned area, fuel availability and combustion completeness. VIIRS high-resolution FRP moreover forms a surprisingly good alternative for burned area as long as cloud obscuration is limited (see van Wees et al., 2022, PhD thesis and as used in FINNv2.5). The NRT fire model would provide first-guess carbon loss, as well as sources of co-emitted species to the CO_2MVS. This preserves the biogeochemical details encapsulated in GFED, while delivering the NRT capacity needed in CO_2MVS and NWP forecasts.

Along a similar vein, EFs in savannas were machine-learned based on observations and various global weather variables from ERA5, or derived indices (Vernooij et al 2023, PhD thesis). A trained model combined with the NWP variables from IFS would allow more dynamic EFs to quickly be available in the CO_2MVS and given the large amount of new EF data in temperate regions there is potential to introduce dynamic emission factors beyond only the savanna biome.

(2) is the inclusion of biomass burning carbon loss in the longer-term reanalyses of the CO_2MVS. Rather than machine-learned emissions, here a more complete description of the carbon pools and their coupling to the state of the land-surface can be leveraged. Fuel availability and consumption depend on the vegetation state with a large hysteresis because of seasonal growth (grasses), seasonal moisture balances (grasses, temperate forests), and even decadal management (standing stocks and litter). Emissions of CO_2, aerosols, and CO depend on combustion completeness and emission factors that similarly vary with weather conditions. And the post-fire state of the landscape in terms of remaining carbon stocks, ensuing regrowth, but also the surface energy balance impact NWP. Such variables can be co-constrained using the ECLand framework to simulate vegetation state (carbon stocks, labile pools, litter, wetness) and surface characteristics (temperature, moisture, greenness).

The design of a biomass burning model that provides these couplings should furthermore account strongly for small fires, which have proven to double burned area globally and possibly add about 50% to total carbon emissions (Chen et al., 2023). Given that VIIRS provides excellent capabilities to detect also these smaller fires an updated fire model in CAMS will provide more realistic emission estimates, also in NRT. They can also contribute heavily to local air pollution, and investments in fire modelling thus offer synergy with developments in CAMS.

An outlook on such expanded fire emissions MVS capacity, beyond that presented based on our CO/CO$_2$ modelling efforts, is provided below.

5.1 Other observational constraints

CO observations, especially space-based, have demonstrated capacity to constrain fire carbon emissions (Zheng et al., 2021; Naus et al., 2022) derived from biogeochemical modelling and observations of burned area or FRP. Mostly, observations from MOPITT and IASI suggest higher emission totals globally. TROPOMI CO has been used mostly in regional studies so far (Velde et al., 2021) but will likely become the main source of XCO data for the post-2017 era. Its smaller footprint will likely help to better filter retrievals affected by smoke and aerosols, of which the influence on retrievals closest to large sources is unknown also for the coarser instruments used thus far. TROPOMI additionally allows retrievals of formaldehyde (HCHO) which can help to constrain the VOC-derived production of CO, which we demonstrated here to be a significant source in the CO-budget, with uncertainties that can impact biomass burning emission estimates from XCO. Whether the VOC-HCHO-CO relation must be modeled in full-chemistry, or if it can be machine-learned and parameterized is a question for follow-up research.

Similar efforts to parameterize the NO$_2$-CO-CO$_2$ relationships in biomass burning plumes are underway, for example in the HE CORSO project. First results have suggested that simulating the NO$_2$ lifetime at coarse model resolutions remains a bottleneck. Global simulations at ~40km resolution insufficiently captured the plume lifetime to use emission ratios from NO2/NO and CO$_2$/CO derived from satellite products. In WP4 of CoCO$_2$ it was similarly demonstrated that NOx chemistry in plumes leads to strongly non-linear tracer ratios at scales of 0.1-10km. This is mostly below the resolution targeted with the CO$_2$-MVS, as well as the resolution of TROPOMI and CO$_2$-M. It is likely that the interpretation of NOx from fires thus requires other modelling approaches, but this was not investigated under this Deliverable.

5.2 Data assimilation

To independently estimate the land-use change carbon sources in the Copernicus CO$_2$MVS, we foresee two pathways:

(1) is using the ***daily operational*** system in which the atmospheric state of CO and CO$_2$ are adjusted together with the surface emissions of CO from fires within the time span of the 24-hour window and the background covariance matrix spanning at least 3 days (based on our experiences with a 3-day window this seems a robust span). The driver data will be mostly TROPOMI XCO in combination with VIIRS Active Fires to optimize biomass burning CO emissions. These are converted to carbon emissions using machine-learned fuel consumption and EFs driven by NWP variables. Prior fire emissions are based on first-guess estimates derived from machine-learning of emissions from a full biogeochemical model. Small fires are accounted for through a similar training on existing datasets. Fire carbon release does not directly impact the land-surface characteristics (albedo, LAI, carbon stocks, vegetation type). CO production from CH$_4$ is done online using fixed OH fields from CAMS. Other terms of the CO budget (fossil emissions, NMHC-production) are prescribed from pre-calculated climatologies taken from CAMS or from a similar large-scale chemistry model.

(2) is an ***annual reanalysis*** of land-use change emissions. In addition to XCO (TROPOMI, MOPITT, and IASI) this reanalysis uses well-calibrated surface and free tropospheric flask sample CO observations. Fire emissions are modeled based on biogeochemical models that track carbon stocks and fuel availability as well as wetness, preferably within ECLand. Small fires (i.e., below 300m in size and detected from hi-res visible imagery) are explicitly included in these first guess estimates. The DA window is extended to at least 3 weeks (based on the chemical lifetime and transport time in/from tropical regions), with the statevector containing daily CO emissions from fires as well as weekly mean EFs across various large PFT's. Smaller scale EF-variability is modeled based on ECLand and NWP variables. Fires affect carbon

stocks and hence regrowth in ECLand, as well as vegetation type, albedo, and LAI during the reanalysis. Once sufficient good quality XCO_2 data is available (e.g. from CO_2M), it can additionally inform on carbon fire emissions in this framework. Other parts of the CO budget are co-optimized in the reanalysis to make sure that the global budget closes well.

Validation of both can be against not used flask, campaign, or satellite data of CO and CO_2, and possibly against NO_2 and formaldehyde on larger scales. A promising avenue is also Aerosol Optical Depth, and possibly data from upcoming biomass satellite datasets. Finally, we mention that alternative estimates performed with other transport models, and different DA approaches would help for continuing R&D on the CO_2-MVS.

6 References

Akagi, S. K., Yokelson, R. J., Wiedinmyer, C., Alvarado, M. J., Reid, J. S., Karl, T., Crounse, J. D., & Wennberg, P. O. (2011). Emission factors for open and domestic biomass burning for use in atmospheric models. *Atmospheric Chemistry and Physics*, *11*(9), 4039–4072. https://doi.org/10.5194/acp-11-4039-2011

Alencar, Ane, Nepstad, Daniel, & Diaz, Mariadel Carmen Vera. (2006). Forest Understory Fire in the Brazilian Amazon in ENSO and Non-ENSO Years: Area Burned and Committed Carbon Emissions. *Earth Interactions*, *10*(6), 1–17. https://doi.org/10.1175/ei150.1

Andreae, M. O., & Merlet, P. (2001). Emission of trace gases and aerosols from biomass burning. *Global Biogeochemical Cycles*, *15*(4), 955. https://doi.org/10.1029/2000gb001382

Balsamo, Gianpaolo, Engelen, Richard, Thiemert, Daniel, Agusti-Panareda, Anna, Bousserez, Nicolas, Broquet, Grégoire, Brunner, Dominik, Buchwitz, Michael, Chevallier, Frédéric, Choulga, Margarita, Gon, Hugo Denier Van Der, Florentie, Liesbeth, Haussaire, Jean-Matthieu, Janssens-Maenhout, Greet, Jones, Matthew W., Kaminski, Thomas, Krol, Maarten, Quéré, Corinne Le, Marshall, Julia, … Scholze, Marko. (2021). The CO2 Human Emissions (CHE) Project: First Steps Towards a European Operational Capacity to Monitor Anthropogenic CO2 Emissions. *Frontiers in Remote Sensing*, *2*, 707247. https://doi.org/10.3389/frsen.2021.707247

Basso, L. S., Wilson, C., Chipperfield, M. P., Tejada, G., Cassol, H. L. G., Arai, E., Williams, M., Smallman, T. L., Peters, W., Naus, S., Miller, J. B., & Gloor, M. (2023). Atmospheric CO$_2$ inversion reveals the Amazon as a minor carbon source caused by fire emissions, with forest uptake offsetting about half of these emissions. *Atmospheric Chemistry and Physics*, *23*(17), 9685–9723. https://doi.org/10.5194/acp-23-9685-2023

Brando, P. M., Soares-Filho, B., Rodrigues, L., Assunção, A., Morton, D., Tuchschneider, D., Fernandes, E. C. M., Macedo, M. N., Oliveira, U., & Coe, M. T. (2020). The gathering firestorm in southern Amazonia. *Science Advances*, *6*(2), eaay1632. https://doi.org/10.1126/sciadv.aay1632

Brando, Paulo, Macedo, Marcia, Silvério, Divino, Rattis, Ludmila, Paolucci, Lucas, Alencar, Ane, Coe, Michael, & Amorim, Cristina. (2020). Amazon wildfires: Scenes from a foreseeable disaster. *Flora*, *268*, 151609. https://doi.org/10.1016/j.flora.2020.151609

Byrne, Brendan, Baker, David F., Basu, Sourish, Bertolacci, Michael, Bowman, Kevin W., Carroll, Dustin, Chatterjee, Abhishek, Chevallier, Frédéric, Ciais, Philippe, Cressie, Noel, Crisp, David, Crowell, Sean, Deng, Feng, Deng, Zhu, Deutscher, Nicholas M., Dubey, Manvendra K., Feng, Sha, García, Omaira E., Griffith, David W. T., … Zeng, Ning. (2023). National CO2 budgets (2015–2020) inferred from atmospheric CO2 observations in support of the global stocktake. *Earth System Science Data*, *15*(2), 963–1004. https://doi.org/10.5194/essd-15-963-2023

Chen, Yang, Hall, Joanne, Wees, Dave van, Andela, Niels, Hantson, Stijn, Giglio, Louis, Werf, Guido R. van der, Morton, Douglas C., & Randerson, James T. (2023). Multi-decadal trends and variability in burned area from the fifth version of the Global Fire Emissions Database (GFED5). *Earth System Science Data*, *15*(11), 5227–5259. https://doi.org/10.5194/essd-15-5227-2023

Crowell, Sean, Baker, David, Schuh, Andrew, Basu, Sourish, Jacobson, Andrew R., Chevallier, Frederic, Liu, Junjie, Deng, Feng, Feng, Liang, McKain, Kathryn, Chatterjee, Abhishek, Miller, John B., Stephens, Britton B., Eldering, Annmarie, Crisp, David, Schimel, David, Nassar, Ray, O'Dell, Christopher W., Oda, Tomohiro, … Jones, Dylan B. A. (2019). The 2015–2016 carbon cycle as seen from OCO-2 and the global in situ network. *Atmospheric Chemistry and Physics*, *19*(15), 9797–9831. https://doi.org/10.5194/acp-19-9797-2019

Dasari, Sanjeev, Andersson, August, Popa, Maria E., Röckmann, Thomas, Holmstrand, Henry, Budhavant, Krishnakant, & Gustafsson, O.¨ Rjan. (2021). Observational Evidence of Large Contribution from Primary Sources for Carbon Monoxide in the South Asian Outflow. *Cite This: Environ. Sci. Technol*, *2022*(1), 165–174. https://doi.org/10.1021/acs.est.1c05486

Deng, Z., Ciais, P., Tzompa-Sosa, Z. A., Saunois, M., Qiu, C., Tan, C., Sun, T., Ke, P., Cui, Y., Tanaka, K., Lin, X., Thompson, R. L., Tian, H., Yao, Y., Huang, Y., Lauerwald, R., Jain, A. K., Xu, X., Bastos, A., … Chevallier, F. (2022). Comparing national greenhouse gas budgets reported in UNFCCC inventories against atmospheric inversions. *Earth System Science Data*, *14*(4), 1639–1675. https://doi.org/10.5194/essd-14-1639-2022

Freitas, S. R., Longo, K. M., Dias, M. A. F. Silva, Chatfield, R., Dias, P. Silva, Artaxo, P., Andreae, M. O., Grell, G., Rodrigues, L. F., Fazenda, A., & Panetta, J. (2009). The Coupled Aerosol and Tracer Transport model to the Brazilian developments on the Regional Atmospheric Modeling System (CATT-BRAMS) – Part 1: Model description and evaluation. *Atmospheric Chemistry and Physics*, *9*(8), 2843–2861. https://doi.org/10.5194/acp-9-2843-2009

Friedlingstein, Pierre, O'Sullivan, Michael, Jones, Matthew W., Andrew, Robbie M., Bakker, Dorothee C. E., Hauck, Judith, Landschützer, Peter, Quéré, Corinne Le, Luijkx, Ingrid T., Peters, Glen P., Peters, Wouter, Pongratz, Julia, Schwingshackl, Clemens, Sitch, Stephen, Canadell, Josep G., Ciais, Philippe, Jackson, Robert B., Alin, Simone R., Anthoni, Peter, … Zheng, Bo. (2023). Global Carbon Budget 2023. *Earth System Science Data*, *15*(12), 5301–5369. https://doi.org/10.5194/essd-15-5301-2023

Ganzeveld, L., Lelieveld, Jos, Dentener, Frank, Krol, Maarten C., & Roelofs, G. (2002). Atmosphere-biosphere trace gas exchanges simulated with a single-column model. *Journal Of Geophysical Research-Oceans And Atmospheres*, *107*(D16).

Gatti, Luciana V., Cunha, Camilla L., Marani, Luciano, Cassol, Henrique L. G., Messias, Cassiano Gustavo, Arai, Egidio, Denning, A. Scott, Soler, Luciana S., Almeida, Claudio, Setzer, Alberto, Domingues, Lucas Gatti, Basso, Luana S., Miller, John B., Gloor, Manuel, Correia, Caio S. C., Tejada, Graciela, Neves, Raiane A. L., Rajao, Raoni, Nunes, Felipe, … Machado, Guilherme B. M. (2023). Increased Amazon carbon emissions mainly from decline in law enforcement. *Nature*, *621*(7978), 318–323. https://doi.org/10.1038/s41586-023-06390-0

Giglio, Louis, Boschetti, Luigi, Roy, David P., Humber, Michael L., & Justice, Christopher O. (2018). The Collection 6 MODIS burned area mapping algorithm and product. *Remote Sensing of Environment*, *217*, 72–85. https://doi.org/10.1016/j.rse.2018.08.005

Giglio, Louis, Schroeder, Wilfrid, & Justice, Christopher O. (2016). The collection 6 MODIS active fire detection algorithm and fire products. *Remote Sensing of Environment*, *178*, 31–41. https://doi.org/10.1016/j.rse.2016.02.054

Giuseppe, Francesca Di, Rémy, Samuel, Pappenberger, Florian, & Wetterhall, Fredrik. (2018). Using the Fire Weather Index (FWI) to improve the estimation of fire emissions from fire radiative power (FRP) observations. *Atmospheric Chemistry and Physics*, *18*(8), 5359–5370. https://doi.org/10.5194/acp-18-5359-2018

Granier, Claire, Bessagnet, Bertrand, Bond, Tami, D'Angiola, Ariela, Gon, Hugo Denier van der, Frost, Gregory J., Heil, Angelika, Kaiser, Johannes W., Kinne, Stefan, Klimont, Zbigniew, Kloster, Silvia, Lamarque, Jean-François, Liousse, Catherine, Masui, Toshihiko, Meleux, Frederik, Mieville, Aude, Ohara, Toshimasa, Raut, Jean-Christophe, Riahi, Keywan, … Vuuren, Detlef P. van. (2011). Evolution of anthropogenic and biomass burning emissions of air pollutants at global and regional scales during the 1980–2010 period. *Climatic Change*, *109*(1–2), 163. https://doi.org/10.1007/s10584-011-0154-1

Grassi, Giacomo, Schwingshackl, Clemens, Gasser, Thomas, Houghton, Richard A., Sitch, Stephen, Canadell, Josep G., Cescatti, Alessandro, Ciais, Philippe, Federici, Sandro, Friedlingstein, Pierre, Kurz, Werner A., Sanchez, Maria J. Sanz, Viñas, Raúl Abad, Alkama, Ramdane, Bultan, Selma, Ceccherini, Guido, Falk, Stefanie, Kato, Etsushi, Kennedy, Daniel, … Pongratz, Julia. (2023). Harmonising the land-use flux estimates of global models and national inventories for 2000–2020. *Earth System Science Data*, *15*(3), 1093–1114. https://doi.org/10.5194/essd-15-1093-2023

Haynes, K D, Baker, I. T., Denning, A. S., Stöckli, R., Schaefer, K., Lokupitiya, E. Y., & Haynes, J. M. (2019). Representing Grasslands Using Dynamic Prognostic Phenology Based on Biological Growth Stages: 1. Implementation in the Simple Biosphere Model (SiB4). *Journal of Advances in Modeling Earth Systems*, *11*(12), 4423–4439. https://doi.org/10.1029/2018ms001540

Haynes, Katherine D, Baker, Ian T., Denning, A. Scott, Wolf, Sebastian, Wohlfahrt, GEORG, Kiely, Gerard, Minaya, Renee C., & Haynes, John M. (2019). Representing Grasslands Using Dynamic Prognostic Phenology Based on Biological Growth Stages: Part 2. Carbon Cycling. *Journal of Advances in Modeling Earth Systems*, *11*(12), 4440–4465. https://doi.org/10.1029/2018ms001541

Hersbach, Hans, Bell, Bill, Berrisford, Paul, Hirahara, Shoji, Horányi, András, Muñoz-Sabater, Joaquín, Nicolas, Julien, Peubey, Carole, Radu, Raluca, Schepers, Dinand, Simmons, Adrian, Soci, Cornel, Abdalla, Saleh, Abellan, Xavier, Balsamo, Gianpaolo, Bechtold, Peter, Biavati, Gionata, Bidlot, Jean, Bonavita, Massimo, … Thépaut, Jean-Noël. (2020). The ERA5 global reanalysis. *Quarterly Journal of the Royal Meteorological Society*, *146*(730), 1999–2049. https://doi.org/10.1002/qj.3803

Huijnen, V., Williams, J., Weele, M. van, Noije, T. van, Krol, M., Dentener, F., Segers, A., Houweling, S., Peters, Wouter, Laat, J. de, Boersma, F., Bergamaschi, P., Velthoven, P. van, Sager, P. Le, Eskes, H., Alkemade, F., Scheele, R., elec, P. N. ed, & atz, H. W. P. (2010). The global chemistry transport model TM5: description and evaluation of the tropospheric chemistry version 3.0. *Geoscientific Model Development*, *3*(2), 445–473. https://doi.org/10.5194/gmd-3-445-2010

Inness, Antje, Ades, Melanie, Agustí-Panareda, Anna, Barré, Jérôme, Benedictow, Anna, Blechschmidt, Anne-Marlene, Dominguez, Juan Jose, Engelen, Richard, Eskes, Henk, Flemming, Johannes, Huijnen, Vincent, Jones, Luke, Kipling, Zak, Massart, Sebastien, Parrington, Mark, Peuch, Vincent-Henri, Razinger, Miha, Remy, Samuel, Schulz, Michael, & Suttie, Martin. (2019). The CAMS reanalysis of atmospheric composition. *Atmospheric Chemistry and Physics*, *19*(6), 3515–3556. https://doi.org/10.5194/acp-19-3515-2019

Jones, Matthew W., Andrew, Robbie M., Peters, Glen P., Janssens-Maenhout, Greet, De-Gol, Anthony J., Ciais, Philippe, Patra, Prabir K., Chevallier, Frederic, & Quéré, Corinne Le. (2021). Gridded fossil CO2 emissions and related O2 combustion consistent with national inventories 1959–2018. *Scientific Data*, *8*(1), 2. https://doi.org/10.1038/s41597-020-00779-6

Kahn, Ralph A., Chen, Yang, Nelson, David L., Leung, Fok-Yan, Li, Qinbin, Diner, David J., & Logan, Jennifer A. (2008). Wildfire smoke injection heights: Two perspectives from space. *Geophysical Research Letters*, *35*(4), L04809. https://doi.org/10.1029/2007gl032165

Kaiser, J. W., Heil, A., Andreae, M. O., Benedetti, A., Chubarova, N., Jones, L., Morcrette, J. J., Razinger, M., Schultz, M. G., Suttie, M., & Werf, G. R. van der. (2012). Biomass burning emissions estimated with a global fire assimilation system based on observed fire radiative power. *Biogeosciences*, *9*(1), 527–554. https://doi.org/10.5194/bg-9-527-2012

Koren, Gerbrand. (2020). *Constraining the exchange of carbon dioxide over the Amazon : New insights from stable isotopes, remote sensing and inverse modeling*. https://doi.org/10.18174/524771

Krol, M., Peters, W., Hooghiemstra, P., George, M., Clerbaux, C., Hurtmans, D., McInerney, D., Sedano, F., Bergamaschi, P., Hajj, M. El, Kaiser, J. W., Fisher, D., Yershov, V., & Muller, J. P. (2013). How much CO was emitted by the 2010 fires around Moscow? *Atmospheric Chemistry and Physics*, *13*, 4737–4747. http://www.atmos-chem-phys.net/13/4737/2013/acp-13-4737-2013.pdf

Krol, Maarten C., Peters, Wouter, Berkvens, P., & Botchev, M. (2001). *A new algorithm for two-way nesting in global models: Principles and Applications*. http://www.google.com/search?client=safari&rls=en&q=A+new+algorithm+for+two-way+nesting+in+global+models:+Principles+and+Applications&ie=UTF-8&oe=UTF-8

Laan-Luijkx, I. T. van der, Velde, I. R. van der, Veen, E. van der, Tsuruta, A., Stanislawska, K., Babenhauserheide, A., Zhang, H. F., Liu, Y., He, W., Chen, H., Masarie, K. A., Krol, M. C., & Peters, Wouter. (2017). The CarbonTracker Data Assimilation Shell (CTDAS) v1.0: implementation and global carbon balance 2001–2015. *GMD*, *10*(7), 2785–2800. https://doi.org/10.5194/gmd-10-2785-2017

Leeuwen, T. T. van, Peters, Wouter, Krol, M. C., & Werf, G. R. van der. (2013). Dynamic biomass burning emission factors and their impact on atmospheric CO mixing ratios. *Journal Of Geophysical Research-Atmospheres*, *118*(12), 6797–6815. https://doi.org/10.1002/jgrd.50478

Leeuwen, T. T. van, Werf, G. R. van der, Hoffmann, A. A., Detmers, R. G., Rücker, G., French, N. H. F., Archibald, S., Jr., J. A. Carvalho, Cook, G. D., Groot, W. J. de, Hély, C., Kasischke, E. S., Kloster, S., McCarty, J. L., Pettinari, M. L., Savadogo, P., Alvarado, E. C., Boschetti, L., Manuri, S., … Trollope, W. S. W. (2014). Biomass burning fuel consumption rates: a field measurement database. *Biogeosciences*, *11*(24), 7305–7329. https://doi.org/10.5194/bg-11-7305-2014

Leguijt, Gijs, Maasakkers, Joannes D., Gon, Hugo A. C. Denier Van Der, Segers, Arjo J., Borsdorff, Tobias, & Aben, Ilse. (2023). Quantification of carbon monoxide emissions from African cities using TROPOMI. *Atmospheric Chemistry and Physics*, *23*, 8899–8919. https://doi.org/10.5194/acp-23-8899-2023

Lorente, A., Boersma, K. F., Eskes, H. J., Veefkind, J. P., Geffen, J. H. G. M. van, Zeeuw, M. B. de, Gon, H. A. C. Denier van der, Beirle, S., & Krol, M. C. (2019). Quantification of nitrogen oxides emissions from build-up of pollution over Paris with TROPOMI. *Scientific Reports*, *9*(1), 20033. https://doi.org/10.1038/s41598-019-56428-5

Martin, M. Val, Logan, J. A., Kahn, R. A., Leung, F. Y., Nelson, D. L., & Diner, D. J. (2010). Smoke injection heights from fires in North America: analysis of 5 years of satellite observations. *Atmospheric Chemistry and Physics*, *10*, 1491–1510. http://adsabs.harvard.edu/abs/2010ACP....10.1491M

McGrath, Matthew J., Petrescu, Ana Maria Roxana, Peylin, Philippe, Andrew, Robbie M., Matthews, Bradley, Dentener, Frank, Balkovič, Juraj, Bastrikov, Vladislav, Becker, Meike, Broquet, Gregoire, Ciais, Philippe, Fortems-Cheiney, Audrey, Ganzenmüller, Raphael, Grassi, Giacomo, Harris, Ian, Jones, Matthew, Knauer, Jürgen, Kuhnert, Matthias, Monteil, Guillaume, … Walther, Sophia. (2023). The consolidated European synthesis of CO2 emissions and removals for the European Union and United Kingdom: 1990–2020. *Earth System Science Data*, *15*(10), 4295–4370. https://doi.org/10.5194/essd-15-4295-2023

Morton, D. C., Page, Y. Le, DeFries, R., Collatz, G. J., & Hurtt, G. C. (2013). Understorey fire frequency and the fate of burned forests in southern Amazonia. *Philosophical Transactions of the Royal Society B: Biological Sciences*, *368*(1619), 20120163. https://doi.org/10.1098/rstb.2012.0163

Myriokefalitakis, S., Daskalakis, N., Gkouvousis, A., Hilboll, A., Noije, T. van, Williams, J. E., Sager, P. Le, Huijnen, V., Houweling, S., Bergman, T., Nüß, J. R., Vrekoussis, M., Kanakidou, M., & Krol, M. C. (2020). Description and evaluation of a detailed gas-phase chemistry scheme in the TM5-MP global chemistry transport model (r112). *Geoscientific Model Development*, *13*, 5507–5548. https://gmd.copernicus.org/articles/13/5507/2020/gmd-13-5507-2020.pdf

Naus, S., Domingues, L. G., Krol, M., Luijkx, I. T., Gatti, L. V., Miller, J. B., Gloor, E., Basu, S., Correia, C., Koren, G., Worden, H. M., Flemming, J., Pétron, G., & Peters, W. (2022). Sixteen years of MOPITT satellite data strongly constrain Amazon CO fire emissions. *Atmospheric Chemistry and Physics*, *22*(22), 14735–14750. https://doi.org/10.5194/acp-22-14735-2022

Naus, Stijn, A., Montzka, S., K., Patra, P., & C., Krol, M. (2021). A three-dimensional-model inversion of methyl chloroform to constrain the atmospheric oxidative capacity. *Atmospheric Chemistry and Physics*, *21*(6), 4809. https://doi.org/10.5194/acp-21-4809-2021

Nepstad, Daniel, Carvalho, Georgia, Barros, Ana Cristina, Alencar, Ane, Capobianco, João Paulo, Bishop, Josh, Moutinho, Paulo, Lefebvre, Paul, Silva, Urbano Lopes, & Prins, Elaine. (2001). Road paving, fire regime feedbacks, and the future of Amazon forests. *Forest Ecology and Management*, *154*(3), 395–407. https://doi.org/10.1016/s0378-1127(01)00511-4

Obermeier, Wolfgang A., Schwingshackl, Clemens, Bastos, Ana, Conchedda, Giulia, Gasser, Thomas, Grassi, Giacomo, Houghton, Richard A., Tubiello, Francesco N., Sitch, Stephen, & Pongratz, Julia. (2023). Country-level estimates of gross and net carbon fluxes from land use, land-use change and forestry. *Earth System Science Data Discussions*, *2023*, 1–58. https://doi.org/10.5194/essd-2023-281

Peiro, Hélène, Crowell, Sean, & III, Berrien Moore. (2022). Optimizing Four Years of CO_2 Biospheric Fluxes from OCO-2 and in situ data in TM5: Fire Emissions from GFED and Inferred from MOPITT CO data. *Atmospheric Chemistry and Physics Discussions*, *2022*, 1–58. https://doi.org/10.5194/acp-2022-120

Peters, Wouter, Jacobson, Andrew R., Sweeney, Colm, Andrews, Arlyn E., Conway, Thomas J., Masarie, Kenneth, Miller, John B., Bruhwiler, Lori M. P., Petron, Gabrielle, Hirsch, Adam I., Worthy, Douglas E. J., Werf, Guido R. van der, Randerson, James T., Wennberg, Paul O., Krol, Maarten C., & Tans, Pieter P. (2007). An atmospheric perspective on North American carbon dioxide exchange: CarbonTracker. *Proceedings of the National Academy of Sciences*, *104*(48), 18925–18930. https://doi.org/10.1073/pnas.0708986104

Randerson, J. T., Chen, Y., Werf, G. R., Rogers, B. M., & Morton, D. C. (2012). Global burned area and biomass burning emissions from small fires. *Journal of Geophysical Research: Atmospheres (1984–2012)*, *117*(G4), G04012. https://doi.org/10.1029/2012jg002128

Randerson, James, Werf, Guido R. van der, Collatz, GJ, Giglio, L., Still, CJ, Kasibhatla, P., Miller, John B., White, JWC, Defries, RS, & Kasischke, ES. (2005). Fire emissions from C3 and C4 vegetation and their influence on interannual variability of atmospheric CO2 and ?13CO2. *Global Biogeochemical Cycles*, *19*(2), 1–13.

Rémy, S., Veira, A., Paugam, R., Sofiev, M., Kaiser, J. W., Marenco, F., Burton, S. P., Benedetti, A., Engelen, R. J., Ferrare, R., & Hair, J. W. (2017). Two global data sets of daily fire emission injection heights since 2003. *Atmospheric Chemistry and Physcis*, *17*, 2921–2942. https://acp.copernicus.org/articles/17/2921/2017/acp-17-2921-2017.pdf

Rigby, Matthew, Montzka, Stephen A., Prinn, Ronald G., White, James W. C., Young, Dickon, O'Doherty, Simon, Lunt, Mark F., Ganesan, Anita L., Manning, Alistair J., Simmonds, Peter G., Salameh, Peter K., Harth, Christina M., Mühle, Jens, Weiss, Ray F., Fraser, Paul J., Steele, L. Paul, Krummel, Paul B., McCulloch, Archie, & Park, Sunyoung. (2017). Role of atmospheric oxidation in recent methane growth. *Proceedings of the National Academy of Sciences*, *114*(21), 5373–5377. https://doi.org/10.1073/pnas.1616426114

Ringsdorf, A., Edtbauer, A., Arellano, J. Vilà-Guerau de, Pfannerstill, E. Y., Gromov, S., Kumar, V., Pozzer, A., Wolff, S., Tsokankunku, A., Soergel, M., Sá, M. O., Araújo, A., Ditas, F., Poehlker, C., Lelieveld, J., & Williams, J. (2023). Inferring the diurnal variability of OH radical concentrations over the Amazon from BVOC measurements. *Scientific Reports 2023 13:1*, *13*, 1–17. https://doi.org/10.1038/s41598-023-41748-4

Schwingshackl, Clemens, Obermeier, Wolfgang A., Bultan, Selma, Grassi, Giacomo, Canadell, Josep G., Friedlingstein, Pierre, Gasser, Thomas, Houghton, Richard A., Kurz, Werner A., Sitch, Stephen, & Pongratz, Julia. (2022). Differences in land-based mitigation estimates reconciled by separating natural and land-use CO2 fluxes at the country level. *One Earth*, *5*(12), 1367–1376. https://doi.org/10.1016/j.oneear.2022.11.009

Smedt, Isabelle De, Pinardi, Gaia, Vigouroux, Corinne, Compernolle, Steven, Bais, Alkis, Benavent, Nuria, Boersma, Folkert, Chan, Ka Lok, Donner, Sebastian, Eichmann, Kai Uwe, Hedelt, Pascal, Hendrick, François, Irie, Hitoshi, Kumar, Vinod, Lambert, Jean Christopher, Langerock, Bavo, Lerot, Christophe, Liu, Cheng, Loyola, Diego, … Roozendael, Michel Van. (2021). Comparative assessment of TROPOMI and OMI formaldehyde observations and validation against MAX-DOAS network column measurements. *Atmospheric Chemistry and Physics*, *21*(16), 12561–12593. https://doi.org/10.5194/acp-21-12561-2021

Sofiev, M., Ermakova, T., & Vankevich, R. (2012). Evaluation of the smoke-injection height from wild-land fires using remote-sensing data. *Atmospheric Chemistry and Physics*, *12*, 1995–2006. https://doi.org/10.5194/acp-12-1995-2012

Sofiev, M., Vankevich, R., Ermakova, T., & Hakkarainen, J. (2013). Global mapping of maximum emission heights and resulting vertical profiles of wildfire emissions. *Atmospheric Chemistry and Physics*, *13*, 7039–7052. https://doi.org/10.5194/acp-13-7039-2013

Suntharalingam, P., Randerson, JT, Krakauer, N., Logan, JA, & Jacob, DJ. (2005). Influence of reduced carbon emissions and oxidation on the distribution of atmospheric CO2: Implications for inversion analyses. *Global Biogeochemical Cycles*, *19*(4), GB4003. http://www.google.com/search?client=safari&rls=en&q=Influence+of+reduced+carbon+emissions+and+oxidation+on+the+distribution+of+atmospheric+CO2:+Implications+for+inversion+analyses&ie=UTF-8&oe=UTF-8

Velde, Ivar R. van der, Miller, John B., Molen, Michiel K. van der, Tans, Pieter P., Vaughn, Bruce H., White, James W. C., Schaefer, Kevin, & Peters, Wouter. (2018). The CarbonTracker Data Assimilation System for CO2 and δ13C (CTDAS-C13 v1.0): retrieving information on land–atmosphere exchange processes. *Geoscientific Model Development*, *11*(1), 283–304. https://doi.org/10.5194/gmd-11-283-2018

Velde, Ivar R. van der, Werf, Guido R. van der, Houweling, Sander, Maasakkers, Joannes D., Borsdorff, Tobias, Landgraf, Jochen, Tol, Paul, Kempen, Tim A. van, Hees, Richard van, Hoogeveen, Ruud, Veefkind, J. Pepijn, & Aben, Ilse. (2021). Vast CO2 release from Australian fires in 2019–2020 constrained by satellite. *Nature*, *597*(7876), 366–369. https://doi.org/10.1038/s41586-021-03712-y

Vernooij, Roland, Eames, Tom, Russel-Smith, Jeremy, Yates, Cameron, Beatty, Robin, Evans, Jay, Edwards, Andrew, Ribeiro, Natasha, Wooster, Martin, Strydom, Tercia, Giongo, Marcos, Borges, Marco, Menezes, Máximo, Barradas, Carol, Wees, Dave van, & Werf, Guido van der. (2023). Dynamic savanna burning emission factors based on satellite data using a machine learning approach. *EGUsphere*, *2023*, 1–31. https://doi.org/10.5194/egusphere-2023-267

Vimont, Isaac J., Turnbull, Jocelyn C., Petrenko, Vasilii V., Place, Philip F., Sweeney, Colm, Miles, Natasha, Richardson, Scott, Vaughn, Bruce H., & White, James W. C. (2019). An improved estimate for the δc and δc signatures of carbon monoxide produced from atmospheric oxidation of volatile organic compounds. *Atmospheric Chemistry and Physics*, *19*, 8547–8562. https://doi.org/10.5194/acp-19-8547-2019

Virgilio, Giovanni Di, Evans, Jason P., Blake, Stephanie A. P., Armstrong, Matthew, Dowdy, Andrew J., Sharples, Jason, & McRae, Rick. (2019). Climate Change Increases the Potential for Extreme Wildfires. *Geophysical Research Letters*, *46*(14), 8517–8526. https://doi.org/10.1029/2019gl083699

Wees, Dave van, Werf, Guido R. van der, Randerson, James T., Rogers, Brendan M., Chen, Yang, Veraverbeke, Sander, Giglio, Louis, & Morton, Douglas C. (2022). Global biomass burning fuel consumption and emissions at 500 m spatial resolution based on the Global Fire Emissions Database (GFED). *Geoscientific Model Development*, *15*(22), 8411–8437. https://doi.org/10.5194/gmd-15-8411-2022

Wells, Kelley C., Millet, Dylan B., Payne, Vivienne H., Deventer, M. Julian, Bates, Kelvin H., Gouw, Joost A. de, Graus, Martin, Warneke, Carsten, Wisthaler, Armin, & Fuentes, Jose D. (2020). Satellite isoprene retrievals constrain emissions and atmospheric oxidation. *Nature 2020 585:7824*, *585*, 225–233. https://doi.org/10.1038/s41586-020-2664-3

Werf, Guido R. van der, Randerson, James T., Giglio, Louis, Leeuwen, Thijs T. van, Chen, Yang, Rogers, Brendan M., Mu, Mingquan, Marle, Margreet J. E. van, Morton, Douglas C., Collatz, G. James, Yokelson, Robert J., & Kasibhatla, Prasad S. (2017). Global fire emissions estimates during 1997–2016. *Earth System Science Data*, *9*(2), 697–720. https://doi.org/10.5194/essd-9-697-2017

Wiedinmyer, C., Akagi, S. K., Yokelson, R. J., Emmons, L. K., Al-Saadi, J. A., Orlando, J. J., & Soja, A. J. (2011). The Fire INventory from NCAR (FINN): a high resolution global model to estimate the emissions from open burning. *Geoscientific Model Development*, *4*(3), 625–641. https://doi.org/10.5194/gmd-4-625-2011

Zhang, S., Zheng, X., Chen, Z., Dan, B., Chen, J. M., Yi, X., Wang, L., & Wu, G. (2014). A Global Carbon Assimilation System using a modified EnKF assimilation method. *Geoscientific Model Development Discussions*, *7*(5), 6519–6547. https://doi.org/10.5194/gmdd-7-6519-2014

Zheng, B, Chevallier, F., Yin, Y., Ciais, P., Fortems-Cheiney, A., Deeter, M. N., Parker, R. J., Wang, Y., Worden, H. M., & Zhao, Y. (2019). Global atmospheric carbon monoxide budget 2000{–}2017 inferred from multi-species atmospheric inversions. *Earth System Science Data*, *11*, 1411–1436. https://essd.copernicus.org/articles/11/1411/2019/essd-11-1411-2019.pdf

Zheng, Bo, Chevallier, Frederic, Yin, Yi, Ciais, Philippe, Fortems-Cheiney, Audrey, Deeter, Merritt N., Parker, Robert J., Wang, Yilong, Worden, Helen M., & Zhao, Yuanhong. (2019). Global atmospheric carbon monoxide budget 2000–2017 inferred from multi-species atmospheric inversions. *Earth System Science Data*, *11*(3), 1411–1436. https://doi.org/10.5194/essd-11-1411-2019

Zhu, Lei, Jacob, Daniel J., Kim, Patrick S., Fisher, Jenny A., Yu, Karen, Travis, Katherine R., Mickley, Loretta J., Yantosca, Robert M., Sulprizio, Melissa P., Smedt, Isabelle De, Abad, Gonzalo González, Chance, Kelly, Li, Can, Ferrare, Richard, Fried, Alan, Hair, Johnathan W., Hanisco, Thomas F., Richter, Dirk, Scarino, Amy Jo, … Wolfe, Glenn M. (2016). Observing atmospheric formaldehyde (HCHO) from space: Validation and intercomparison of six retrievals from four satellites (OMI, GOME2A, GOME2B, OMPS) with SEAC4RS aircraft observations over the southeast US. *Atmospheric Chemistry and Physics*, *16*, 13477–13490. https://doi.org/10.5194/acp-16-13477-2016

Document History

Version	Author(s)	Date	Changes
	Name (Organisation)	dd/mm/yyyy	

Internal Review History

Internal Reviewers	Date	Comments
Name (Organisation)	dd/mm/yyyy	

Estimated Effort Contribution per Partner

Partner	Effort
Organisation	effort in person month
Total	**0**